Simultaneous Identification and Adaptive Torque Control of Permanent Magnet Synchronous Machines

David M. Reed, *Member, IEEE,* Jing Sun, *Fellow, IEEE,* and Heath F. Hofmann, *Senior Member, IEEE*

Abstract—This paper presents an experimentally-verified, Lyapunov-based adaptive control design for permanent magnet synchronous AC machines which exploits overactuation to achieve parameter identification and torque regulation objectives simultaneously. This is achieved by regulating the states of the system (i.e., the stator currents) to the output error-zeroing manifold, along which they are varied to provide excitation for parameter identification. The proposed control law utilizes a combination of adaptively-tuned feedforward and feedback decoupling terms, in addition to proportional feedback, to achieve reference current tracking in the presence of parameter uncertainty. A switching-sigma modification to the adaptive update law is used to ensure robust stability of the closed-loop adaptive system, and excitation for parameter estimation is introduced via the direct-axis current reference input. The resulting controller achieves the simultaneous identification and control objective while providing consistent transient response characteristics with zero steady-state error over a wide range of operating points.

Index Terms—Adaptive Control, Synchronous Motor Drives, Overactuated Systems, Simultaneous Identification and Control.

I. INTRODUCTION

Parameter identification and output regulation are often conflicting objectives, with identification requiring persistently exciting inputs [1] that are rich in harmonics for parameter convergence, while output regulation objectives typically involve tracking a set-point or reference trajectory which does not generate persistently exciting inputs. This trade-off between parameter identification and output regulation objectives makes optimization-based approaches a natural framework for Simultaneous Identification and Control (SIC) methodologies. The "dual control" problem, proposed by Feldbaum in 1960 [2], casts the SIC objective as a stochastic optimal control problem which trades-off minimization of the regulated output error and parameter uncertainty. However, analysis of the dual control problem requires nonlinear stochastic control theory and solutions are difficult, if not impossible, to obtain for all but simple problems [3]. Because of this limitation, there has been a lot of interest in finding approximate (or sub-optimal) approaches to achieving the dual control objective. In

particular, Model Predictive Control (MPC) has been explored as a framework for SIC [4], [5], [6], [7], [8]. While a trade-off is unavoidable for most systems, overactuated[1] systems provide an opportunity to introduce excitation for parameter identification in such a way that it does not perturb regulated outputs. For example, in [9], [10] the authors exploit the "null motion" of an overactuated spacecraft to introduce excitation for parameter identification without disturbing the control objective. Similarly, in [11] overactuation in an experimental electric vehicle is leveraged to provide additional excitation for accurate tire-road friction coefficient estimation.

Permanent Magnet Synchronous Machines (PMSMs), which include both Surface Mount Permanent Magnet (SMPM) and Interior Permanent Magnet (IPM) rotor configurations, are an example of an overactuated system in that there are two inputs, the direct and quadrature-axis voltages, for a single regulated output (i.e., torque for the purposes of this paper). These machines have become a popular choice for many drive applications due to their high torque density and potential for high efficiency. However, variations in the machine parameters due to temperature changes, skin effect, and saturation can detune the transient characteristics of the drive and cause significant steady-state errors in regulated torque [12]. Temperature variations primarily impact the stator resistance, which can increase by as much as 100% [12], and, to a lesser degree, the permanent magnet flux, which has a negative temperature coefficient of around 0.1% per °C for neodymium ($NdFeB$) magnets [13]. In addition to variations with temperature, in the case of high-pole-pair designs and high-speed applications, the electrical frequencies in the stator can reach levels where skin effect begins to cause a noticeable increase in stator resistance.

A wide variety of approaches have been proposed by researchers over the years to address the issue of parameter variation in Permanent Magnet Synchronous Machines (PMSMs). In [14], a nonlinear adaptive controller which achieves asymptotic position tracking using full-state feedback (i.e., current, speed, and position measurements) is presented for SMPM machines, while the approaches presented in [15] and [16] address the position tracking problem when a velocity measurement isn't available (i.e., using only current and position measurements). Adaptive control techniques have even been employed to estimate parameters for extended machine

David M. Reed and Heath F. Hofmann are with the department of Electrical Engineering and Computer Science and Jing Sun is with the department of Naval Architecture and Marine Engineering at the University of Michigan, Ann Arbor, MI 48109 USA (e-mail: davereed@umich.edu; jingsun@umich.edu; hofmann@umich.edu).

---

[1]*Overactuated* systems, in the context of this paper, are systems in which the number of inputs is greater than the number of outputs to be controlled.

models with the goal of minimizing torque ripple in PMSMs [17]. Least Square Estimators (LSEs) have been designed for the purpose of estimating machine parameters online in both closed-loop [18], [19] and open-loop [20], [21] configurations. The approach presented in [18] divides the estimation task into a "fast" LSE for the inductances and a separate "slow" LSE for resistance and torque constant, which are functions of slow thermal variations. In [22], the author uses the gradient (steepest descent) algorithm to adaptively estimate parameter variations, which are modeled as lumped time-varying disturbances. The use of artificial neural networks has been explored as well [23]. Still, Lyapunov-based designs are an attractive approach as they provide some stability assurances as part of the design process [24], [25]. To avoid some of the complexity associated with parameter estimation based on dynamic models, the authors of [26] and [27] develop their parameter estimators using steady-state machine models. These methods, however, do not specifically consider the Simultaneous Identification and Control (SIC) objective; that is, designs which ensure that inputs to the plant are persistently exciting while minimizing the impact of the excitation on the regulated output(s).

This paper presents an experimentally-verified, Lyapunov-based adaptive control design for permanent magnet synchronous AC machines which exploits overactuation to achieve parameter identification and torque regulation objectives simultaneously. We begin by discussing the simultaneous identification and control objective, and the proposed method of regulating states to the output error-zeroing manifold in the context of torque regulation for PMSMs. After reviewing the dynamic PMSM machine model, the derivation and stability proof for the proposed Lyapunov-based adaptive controller is presented. The adaptively-tuned control law utilizes a combination of feedforward and feedback decoupling terms, in addition to proportional feedback, to achieve reference current tracking in the presence of parameter uncertainty. Excitation for parameter estimation is introduced via the direct-axis current reference input. Conditions necessary and sufficient for parameter convergence are discussed, and simulation results verifying the performance of the control design in both ideal and practical scenarios are presented. Challenges which are encountered in experimental implementations are discussed, along with experimental results obtained for a 250 watt surface-mount permanent magnet synchronous machine. Finally, this paper represents a significant extension of our conference paper [28]. Specifically, we have:

1) extended the design to the more general PMSM model;
2) included a more comprehensive discussion of the proposed SIC methodology for overactuated systems;
3) provided a thorough analysis of persistently exciting inputs as well as necessary and sufficient conditions for parameter convergence;
4) updated and expanded the experimental results.

II. SIMULTANEOUS IDENTIFICATION AND CONTROL OBJECTIVE AND METHODOLOGY

In this paper, when we refer to "Simultaneous Identification and Control" or "SIC", we are referring specifically to control designs which ensure that sufficient conditions for accurate parameter identification (i.e., persistently exciting inputs) are maintained in addition to achieving a control objective, such as output regulation. This is in contrast to typical adaptive control designs, which generally guarantee zero steady-state control error, regardless of the accuracy of the estimated parameters. However, in some applications, accurate knowledge of the system parameters is desirable, for example, for condition monitoring, or to guarantee specific transient characteristics. While there are clear advantages to having accurate parameter knowledge, identification and control are typically conflicting objectives, necessitating a trade-off as discussed in the introduction. However, overactuated systems provide an opportunity to achieve both identification and control objectives simultaneously and without compromise, since there is no unique input vector for a given output value.

The SIC design approach demonstrated in this paper on torque regulation in PMSMs is based on constraining the states of the system (i.e., the direct and quadrature-axis stator currents, i_d^r and i_q^r) to a set which corresponds to a particular desired (regulated) output value. Specifically, we are interested in regulating the (unmeasured) electromagnetic torque output of PMSMs, τ, for which the regulated output error is defined as follows:

$$
\begin{aligned}
e_\tau &= \tau^* - \tau, \\
&= \tau^* - h(\vec{\theta}, i_d^r, i_q^r),
\end{aligned}
\tag{1}
$$

where τ^* is the reference torque input and $h(\,\cdot\,) : \mathbb{R}^2 \mapsto \mathbb{R}$ is the nonlinear torque output mapping provided in (4) which is dependent on the parameters, $\vec{\theta}$. Note that e_τ describes a 1-D manifold, i.e., a line, in the two-dimensional (i_d^r, i_q^r) state-space (see Figure 1). We define this output error-zeroing manifold as follows:

$$
\mathcal{M} := \{(i_d^r, i_q^r) \in \mathbb{R}^2 \ : \ e_\tau = \tau^* - h(\vec{\theta}, i_d^r, i_q^r) = 0\}. \tag{2}
$$

Thus, restricting the system state to this manifold ensures that our output regulation objective is achieved, while the non-zero dimension of $\mathcal{M}$ provides space in which the state may vary for identification purposes.

While it is possible to drive the state to points in the set $\mathcal{M}$ with a single input, provided that $\mathcal{M}$ is in the controllable subspace, it is generally not possible (with a single input) to
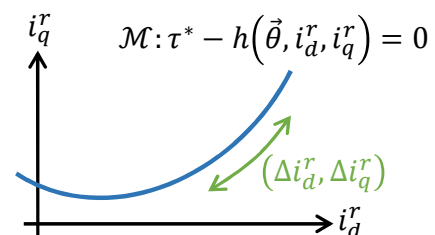

Fig. 1. Depiction of a 1-D manifold in $\mathbb{R}^2$.

vary the state within the set $\mathcal{M}$ without departing for a time, which results in a perturbation of the regulated output. Over-actuation provides additional inputs to the system which may be coordinated in such a way that the state not only converges to $\mathcal{M}$, but also varies within the set, without departing. Recall that the torque regulation problem for PMSMs is overactuated since we have two inputs to the system, v_d^r and v_q^r, but only one "regulated" output, i.e., torque. Thus, for our application, we wish to find an input pair, $(v_d^r, v_q^r)(t)$, such that the states, i_d^r and i_q^r, converge asymptotically to the set $\mathcal{M}$, as defined in (2), while generating sufficient excitation for parameter estimation by varying (i_d^r, i_q^r) within $\mathcal{M}$. This is achieved by designing an adaptive current regulator, developed in Section IV, which ensures asymptotic tracking of filtered reference currents in the presence of parameter uncertainty. The reference currents are computed by specifying a reference torque and a persistently exciting direct-axis current reference and solving the torque output mapping for the quadrature-axis current.

III. FIELD-ORIENTED TWO-PHASE EQUIVALENT DYNAMIC MODEL FOR PMSMS

TABLE I
LIST OF COMMON NOTATION.

Symbol	Description
Electrical Variables	
$v_d^r(t)$	Direct-axis Voltage in Rotor Ref. Frame
$v_q^r(t)$	Quadrature-axis Voltage in Rotor Ref. Frame
$i_d^r(t)$	Direct-axis Current in Rotor Ref. Frame
$i_q^r(t)$	Quadrature-axis Current in Rotor Ref. Frame
R	Stator Winding Resistance
L_d	Direct-axis Stator Self-Inductance
L_q	Quadrature-axis Stator Self-Inductance
Λ_{PM}	Permanent Magnet Flux Linkage
Mechanical Variables	
τ	Three-Phase Electromagnetic Torque
ω_r	Rotor Angular Velocity
$\omega_{re} = \frac{P}{2}\omega_r$	Rotor Electrical Angular Velocity
P	Number of Poles
Special Matrices	
$\mathbf{I}$	Identity Matrix
$\mathbf{0}$	Zero Matrix

Field-oriented control (FOC) [29] and its variants have become the standard for high-performance control of AC machinery and drive systems. By projecting the sinusoidal electrical variables into appropriate rotating reference frames using the Park transform [30], a decoupling of the torque-and-field-generating components of electrical currents is achieved. The resulting field-oriented machine dynamics are analogous to that of a separately excited (field-winding) DC machine, where field-and-torque-generating electrical currents are independently controlled.

The proposed control algorithm is designed around the standard rotor field-oriented two-phase equivalent model for
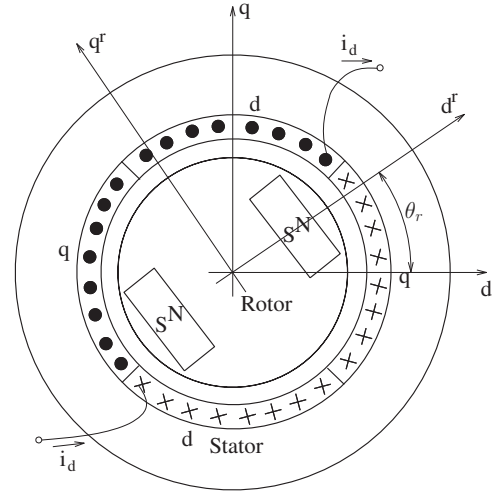

Fig. 2. Cross-section of the two-phase equivalent, two-pole smooth airgap interior-permanent-magnet PMSM machine.

permanent-magnet synchronous machines [31]. This model, and the subsequent control design, are derived under the following assumptions:

A1. The machine to be controlled has a smooth airgap (i.e., slotting effects are neglected), is fed by an ideal voltage source inverter (VSI), and is balanced in its construction such that it can be accurately represented by its 2-phase equivalent model;

A2. Linear magnetics is assumed (i.e., magnetic saturation effects are neglected), and core losses are neglected;

A3. The rotor (electrical) velocity, ω_{re}, is a known (i.e., measured) function of time where $|\omega_{re}|$ and $|\dot{\omega}_{re}|$ are bounded for all $t \geq 0$;

A4. The sampling frequency of the digital implementation is high enough that a continuous-time control design can be sufficiently approximated;

A5. The only uncertain parameters are resistance, R, permanent magnet flux linkage, Λ_{PM}, and the direct and quadrature inductances, L_d and L_q, respectively.

These are common assumptions which are valid under normal operating conditions.

The first three assumptions (**A1** - **A3**) simplify the model and reduce its order, while the last two assumptions (**A4** and **A5**) pertain to the control design and methodology. Under these assumptions, the dynamic model of a PMSM in the rotor reference frame (denoted by the superscript r), in which the direct-axis is aligned with the rotor permanent magnet flux, is given by:

$$L_d \frac{di_d^r}{dt} = -Ri_d^r + \omega_{re} L_q i_q^r + v_d^r,$$
$$L_q \frac{di_q^r}{dt} = -\omega_{re} L_d i_d^r - Ri_q^r + v_q^r - \omega_{re} \Lambda_{PM}, \quad (3)$$

with the *unmeasured* nonlinear torque output mapping

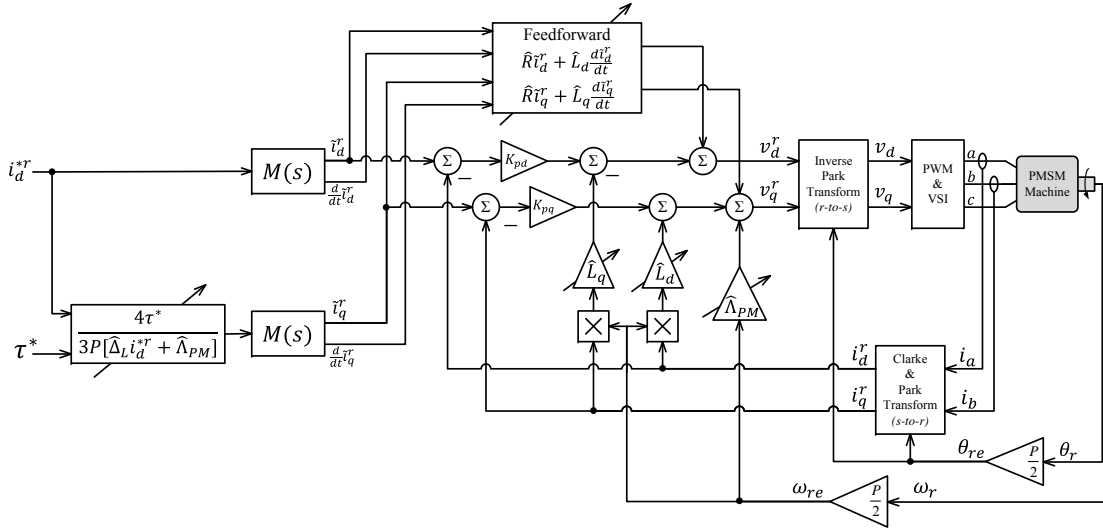$$\tau = \frac{3P}{4} \left[(L_d - L_q) i_d^r + \Lambda_{PM} \right] i_q^r. \quad (4)$$

Fig. 3. Block diagram of the proposed control law.

IV. ADAPTIVE CONTROL DESIGN

A. Reference Current Calculation

Given τ^* and i_d^{*r}, we solve for the reference quadrature current, i_q^{*r}, which is the primary torque generating component of the stator currents:

$$i_q^{*r} = \frac{\tau^*}{\frac{3P}{4}\left(\hat{\Delta}_L i_d^{*r} + \hat{\Lambda}_{PM}\right)}, \tag{5}$$

where the "hat" ($\hat{\ }$) is used to denote estimated parameters and $\hat{\Delta}_L = \hat{L}_d - \hat{L}_q$.

Remark: The expression (5) is well-defined provided that $\hat{\Delta}_L i_d^{*r} + \hat{\Lambda}_{PM} \neq 0$. For this condition (i.e., $\hat{\Delta}_L i_d^{*r} + \hat{\Lambda}_{PM} = 0$) to occur in practice, an impractically large direct-axis current (i.e., one which would likely exceed the current limitations of the machine) and/or extremely erroneous parameter estimates are required, which is impossible due to the presence of a switching-sigma modification used to bound the parameter estimates to reasonable values.

As shown in the next section, derivatives of the reference current trajectories are needed to properly formulate the closed-loop error dynamics, and subsequent Lyapunov-based design, for asymptotic tracking of time-varying signals (i.e., we are looking to *track* signals rather than regulate to a set-point). In this paper, we use reference filters as a convenient way of computing these derivatives online while also ensuring that the voltage commands remain bounded under step changes in the unfiltered reference commands (particularly torque):

$$\tilde{\vec{i}}^r = \{M(s)\}\,\vec{i}^{*r},$$
$$\frac{d}{dt}\tilde{\vec{i}}^r = \{sM(s)\}\,\vec{i}^{*r}, \tag{6}$$

where the "tilde" ($\tilde{\ }$) is used to denote the *filtered* reference currents and $M(s)$ is a stable, minimum phase, strictly proper, unity dc gain, first-order low-pass filter[2]. Note that if the

---

[2] $\{\cdot\}$ denotes a dynamic operator with transfer function "$\cdot$"

---

derivatives of τ^* and i_d^{*r} are bounded and known *a priori*, then the reference filters may be eliminated. Next, we seek an adaptive current-regulating control design which will ensure asymptotic tracking of the filtered reference currents in the presence of parametric uncertainty.

Remark: Note that the adaptive current-regulating control design which follows only guarantees that the measured stator currents, $\vec{i}^r$, asymptotically track the *filtered* reference currents, $\tilde{\vec{i}}^r$. The unfiltered reference signals, $\vec{i}^{*r}$, and $\tilde{\vec{i}}^r$ (and subsequently, $\vec{i}^r$) will differ accordingly, as determined by the frequency response characteristics of the user designed LTI reference filter, $M(s)$.

B. Adaptive Current Regulator

The direct and quadrature stator current errors are defined as follows:

$$e_{id}^r = \tilde{i}_d^r - i_d^r,$$
$$e_{iq}^r = \tilde{i}_q^r - i_q^r. \tag{7}$$

The following control law,

$$v_d^r = \hat{R}\tilde{i}_d^r + \hat{L}_d\frac{d\tilde{i}_d^r}{dt} - \omega_{re}\hat{L}_q i_q^r + K_{pd}e_{id}^r,$$
$$v_q^r = \hat{R}\tilde{i}_q^r + \hat{L}_q\frac{d\tilde{i}_q^r}{dt} + \omega_{re}\hat{L}_d i_d^r + K_{pq}e_{iq}^r + \omega_{re}\hat{\Lambda}_{PM}, \tag{8}$$

where $K_{pd}, K_{pq} > 0$ are constant proportional control gains, is formulated using a combination of feedforward, feedback, and decoupling terms, designed to yield exponentially stable stator current error dynamics (9) under perfect model knowledge (i.e., $\hat{R} = R$, $\hat{L}_d = L_d$, $\hat{L}_q = L_q$, and $\hat{\Lambda}_{PM} = \Lambda_{PM}$):

$$\dot{e}_{id}^r = -\frac{1}{L_d}\left(R + K_{pd}\right)e_{id}^r,$$
$$\dot{e}_{iq}^r = -\frac{1}{L_q}\left(R + K_{pq}\right)e_{iq}^r. \tag{9}$$

Note that the use of a derivative term in the feedforward portion of the control law (8) does not amplify noise, as the

differential operator is acting on reference signals (6) which are free of noise.

However, when the parameters R, L_d, L_q, and Λ_{PM} are not well known, one can show that the closed-loop error dynamics are given by:

$$\dot{\vec{e}}_i^r = \mathbf{L}^{-1}\mathbf{\Phi}^\top \vec{e}_\theta - (R\mathbf{I} + \mathbf{K}_p)\,\mathbf{L}^{-1}\vec{e}_i^r, \qquad (10)$$

where $\mathbf{K}_p = \mathrm{diag}\,[K_{pd}, K_{pq}]$ is a diagonal matrix of the proportional control gains, $\mathbf{L} = \mathrm{diag}\,[L_d, L_q]$ is a diagonal matrix of the direct and quadrature axis self-inductance, $\vec{e}_i^r = \begin{bmatrix} e_{id}^r & i_{iq}^r \end{bmatrix}^\top$ is the stator current error vector, and $\vec{e}_\theta = \begin{bmatrix} e_R & e_{L_d} & e_{L_q} & e_\Lambda \end{bmatrix}^\top$ is the parameter error vector, with $e_R = R - \hat{R}$, $e_{L_d} = L_d - \hat{L}_d$, $e_{L_q} = L_q - \hat{L}_q$, and $e_\Lambda = \Lambda_{PM} - \hat{\Lambda}_{PM}$. Finally, the regressor matrix, $\mathbf{\Phi}$, in (10) is given by

$$\mathbf{\Phi}^\top(t, \vec{e}_i^r) = \begin{bmatrix} \vec{\phi}_d^\top \\ \vec{\phi}_q^\top \end{bmatrix} = \begin{bmatrix} \tilde{i}_d^r & \frac{d}{dt}\tilde{i}_d^r & -\omega_{re}i_q^r & 0 \\ \tilde{i}_q^r & \omega_{re}i_d^r & \frac{d}{dt}\tilde{i}_q^r & \omega_{re} \end{bmatrix}. \qquad (11)$$

To stabilize (10) and ensure that our simultaneous identification and control objectives are achieved in the presence of parameter uncertainty, adaptation is required. A block diagram of the proposed controller implementation is given in Figure 3, where the crossing arrows behind blocks symbolize portions of the controller which are tuned by the adaptation. To derive the adaptive update law, a Lyapunov stability analysis of the closed-loop system is performed. The adaptive law is then selected such that it makes the Lyapunov function monotonically decreasing, thereby guaranteeing closed-loop stability of the controlled system. The following Lyapunov function candidate forms the basis of the derivation:

$$V(\vec{e}_i^r, \vec{e}_\theta) = \frac{1}{2}\left(\vec{e}_i^{r\top}\mathbf{L}\vec{e}_i^r + \vec{e}_\theta^\top\mathbf{\Gamma}^{-1}\vec{e}_\theta\right), \qquad (12)$$

where $\mathbf{\Gamma} = \mathbf{\Gamma}^\top > 0$ is the adaptation gain matrix. The first derivative of (12) with respect to time is given by

$$\dot{V}(\vec{e}_i^r, \vec{e}_\theta) = \vec{e}_i^{r\top}\mathbf{L}\dot{\vec{e}}_i^r + \vec{e}_\theta^\top\mathbf{\Gamma}^{-1}\dot{\vec{e}}_\theta. \qquad (13)$$

Substituting (10) into (13), with some manipulation, yields:

$$\dot{V} = -\vec{e}_i^{r\top}\left[R\mathbf{I} + \mathbf{K}_p\right]\vec{e}_i^r + \vec{e}_\theta^\top\mathbf{\Phi}\vec{e}_i^r + \vec{e}_\theta^\top\mathbf{\Gamma}^{-1}\dot{\vec{e}}_\theta. \qquad (14)$$

It is assumed that the actual machine parameters are changing very slowly, i.e.:

$$\dot{\vec{e}}_\theta = \dot{\vec{\theta}} - \dot{\hat{\vec{\theta}}} \approx -\dot{\hat{\vec{\theta}}}, \qquad (15)$$

where $\hat{\vec{\theta}} = \begin{bmatrix} \hat{R} & \hat{L}_d & \hat{L}_q & \hat{\Lambda}_{PM} \end{bmatrix}^\top$. Finally, the adaptive law is selected as,

$$\dot{\hat{\vec{\theta}}} = \mathbf{\Gamma}\mathbf{\Phi}\vec{e}_i^r, \qquad (16)$$

and so (14) becomes

$$\dot{V}(\vec{e}_i^r, \vec{e}_\theta) = -\vec{e}_i^{r\top}\left[R\mathbf{I} + \mathbf{K}_p\right]\vec{e}_i^r \leq 0. \qquad (17)$$

Therefore, the closed-loop system (3), with control law (8) and adaptation (16), is stable in the sense of Lyapunov [32].

To establish asymptotic convergence of the stator current error (i.e., $\vec{e}_i^r \to 0$ as $t \to \infty$), Barbalat's lemma [32] is used to show that $\dot{V}(\vec{e}_i^r, \vec{e}_\theta) \to 0$ as $t \to \infty$. Note that the preceding

Lyapunov stability analysis has established that $V(\vec{e}_i^r, \vec{e}_\theta)$ is differentiable and has a finite limit as $t \to \infty$. To establish uniform continuity of $\dot{V}(\vec{e}_i^r, \vec{e}_\theta)$ we compute:

$$\ddot{V}(\vec{e}_i^r, \vec{e}_\theta) = -2\vec{e}_i^{r\top}\left[R\mathbf{I} + \mathbf{K}_p\right]\dot{\vec{e}}_i^r, \qquad (18)$$

and note that:

- $\vec{e}_i^r$ and $\vec{e}_\theta$ are bounded from (12) and (17),
- $\tilde{\vec{i}}^r$ and $\frac{d}{dt}\tilde{\vec{i}}^r$ are bounded by design, and so
- $\vec{i}^r = \tilde{\vec{i}}^r - \vec{e}_i^r$ is bounded,

thus $\dot{\vec{e}}_i^r$ is bounded (from inspection of (10)), and so $\ddot{V}(\vec{e}_i^r, \vec{e}_\theta)$ is also bounded. Therefore, from Barbalat's lemma we have that $\dot{V}(\vec{e}_i^r, \vec{e}_\theta) \to 0$ as $t \to \infty$; and so we conclude that the control law (8) with adaptive law (16) renders the system (3) stable in the sense of Lyapunov, with $\vec{e}_i^r \to 0$ as $t \to \infty$.

Lastly, we note that, in practice, our implementation of the adaptive update law (16) includes a "switching σ-modification" [1] for robustness, which acts as a "soft projection", applying a leakage term, σ, to the adaptive law only when a parameter is exceeding an expected limit on its range of variation. A benefit of this modification is that the ideal behavior of the adaptive law is preserved so long as the estimated parameters remain within their acceptable bounds (i.e., $|\hat{\vec{\theta}}_i(t)| < M_{0,i}$).

V. PARAMETER IDENTIFICATION

A. Parameter Convergence

With the controller (8) and adaptive (16) laws presented in the previous section, the closed-loop error dynamics (control and parameter) take the form

$$\begin{aligned} \dot{\vec{e}}_i^r &= \mathbf{L}^{-1}\mathbf{\Phi}^\top(t, \vec{e}_i^r)\vec{e}_\theta - \mathbf{L}^{-1}\left(R\mathbf{I} + \mathbf{K}_p\right)\vec{e}_i^r, \\ \dot{\vec{e}}_\theta &= -\mathbf{\Gamma}\mathbf{\Phi}(t, \vec{e}_i^r)\vec{e}_i^r, \end{aligned} \qquad (19)$$

which may be rewritten as follows

$$\frac{d}{dt}\begin{bmatrix} \vec{e}_i^r \\ \vec{e}_\theta \end{bmatrix} = \begin{bmatrix} \mathbf{A}(t, \vec{e}_i^r) + \mathbf{B}(t, \vec{e}_i^r, \vec{e}_\theta) \\ \mathbf{C}(t, \vec{e}_i^r) \end{bmatrix}, \qquad (20)$$

where $\mathbf{A}(t, \vec{e}_i^r) = -\mathbf{L}^{-1}\left(R\mathbf{I} + \mathbf{K}_p\right)\vec{e}_i^r$, $\mathbf{B}(t, \vec{e}_i^r, \vec{e}_\theta) = \mathbf{L}^{-1}\mathbf{\Phi}^\top\vec{e}_\theta$, and $\mathbf{C}(t, \vec{e}_i^r) = -\mathbf{\Gamma}\mathbf{\Phi}\vec{e}_i^r$. Additionally, we note that the Lyapunov analysis in Section IV establishes Uniform Global Stability (UGS) of the closed-loop system (19). It follows from Theorem 3 in [33] that the origin of the closed-loop system (20) is Uniformly Globally Asymptotically Stable (UGAS) if, and only if, $\mathbf{\Phi}(t, 0)$ is persistently exciting, i.e., there exist $T > 0$, $\alpha_0 > 0$, and $\alpha_1 > 0$ such that,

$$\alpha_1\mathbf{I} \geq \int_t^{t+T} \mathbf{\Phi}(\sigma, 0)\mathbf{\Phi}^\top(\sigma, 0)d\sigma \geq \alpha_0\mathbf{I}, \quad \forall\, t \geq 0. \qquad (21)$$

B. Persistently Exciting Inputs

To determine necessary and sufficient conditions for persistent excitation, and thus for parameter convergence, we will take advantage of the connection between persistent excitation and linear independence of the functions which make up the rows of the regressor matrix. The definition for linear independence of vector-valued functions (of time) is similar to

that of constant vectors (e.g., in $\mathbb{R}^n$) with the difference being that an interval of interest (i.e., the domain) is specified. The definition for linear independence of vector-valued functions is given here for convenience:

Definition 1. (Linear Independence of Functions [34]): *A set of $1 \times p$ real-valued functions, $\vec{f}_i(t)$ where $i = 1, \cdots, n$, is said to be **linearly dependent** on the interval $[t_0, t_1]$ over the field of reals if there exist scalars c_i, not all zero, such that*

$$c_1 \vec{f}_1(t) + c_2 \vec{f}_2(t) + \cdots + c_n \vec{f}_n(t) = 0$$

*for all $t \in [t_0, t_1]$. Otherwise, they are said to be **linearly independent** on the interval $[t_0, t_1]$.*

Naturally, there are a number of theorems which may be used to check whether or not a set of functions is linearly independent. For example, the Grammian matrix may be used:

Theorem 2. (Grammian [34]): *Let $\vec{f}_i(t)$, for $i = 1, 2, \cdots, n$, be $1 \times p$ real-valued continuous functions defined on the interval $[t_1, t_2]$. Let $\mathbf{F}$ be the $n \times p$ matrix with $\vec{f}_i(t)$ as its ith row. Define*

$$\mathbf{W}(t_1, t_2) \triangleq \int_{t_1}^{t_2} \mathbf{F}(t)\mathbf{F}^\top(t)dt$$

*Then $\vec{f}_1(t), \vec{f}_2(t), \cdots, \vec{f}_n(t)$ are **linearly independent** on $[t_1, t_2]$ if, and only if, the $n \times n$ constant Grammian matrix, $\mathbf{W}(t_1, t_2)$, is **positive definite**.*

At this point, the connections between linear independence of the functions which comprise the rows of the regressor matrix, and persistent excitation can be made by noting that the definition of persistent excitation is based on the Grammian matrix. For completeness and easy reference, this connection is summarized in the following theorem:

Theorem 3. *(Linearly Independent Functions and Persistent Excitation): Consider the matrix function $\mathbf{\Phi}(t) : \mathbb{R}_{\geq 0} \mapsto \mathbb{R}^{n \times m}$ where the elements of $\mathbf{\Phi}(t)$ are bounded for all time, t. The regressor matrix $\mathbf{\Phi}(t)$ is **persistently exciting** if, and only if, the rows of $\mathbf{\Phi}(t)$ are **linearly independent** on the interval $[t, t + T]$ for all $t \geq 0$ and some $T > 0$.*

Proof: Follows from the Grammian matrix and its properties and is provided in the Appendix. ⊠

The regressor matrix (11) is a function of the reference signals, $\tilde{i}_d^r$ and $\tilde{i}_q^r$, as well as the states of the system, i_d^r and i_q^r. However, we may rewrite the states in terms of their corresponding reference signals and tracking errors, leading to the following representation of the regressor matrix,

$$\mathbf{\Phi}(t, \vec{e}_i^r) = \mathbf{\Phi}_o(t) + \mathbf{\Phi}_e(t, \vec{e}_i^r),$$

$$= \begin{bmatrix} \tilde{i}_d^r & \tilde{i}_q^r \\ \frac{d}{dt}\tilde{i}_d^r & \omega_{re}\tilde{i}_d^r \\ -\omega_{re}\tilde{i}_q^r & \frac{d}{dt}\tilde{i}_q^r \\ 0 & \omega_{re} \end{bmatrix} + \begin{bmatrix} 0 & 0 \\ 0 & -\omega_{re}e_{id}^r \\ \omega_{re}e_{iq}^r & 0 \\ 0 & 0 \end{bmatrix}.$$

$$(22)$$

Recall that our analysis in Section IV established that the stator current error is bounded (i.e., $\mathbf{\Phi}_e(t, \vec{e}_i^r) \in \mathcal{L}_\infty$) and

goes to zero asymptotically (i.e., $\mathbf{\Phi}_e(t, \vec{e}_i^r) \to 0$ as $t \to \infty$). From Lemma 4.8.3 in [1], it follows that if the matrix $\mathbf{\Phi}_o(t)$ is persistently exciting, then $\mathbf{\Phi}(t, \vec{e}_i^r)$ is persistently exciting. Additionally, we note that from Theorem 3 in [33], it is sufficient to show that $\mathbf{\Phi}(t, 0) \equiv \mathbf{\Phi}_o(t)$ is persistently exciting.

To simplify our analysis, we will conservatively assume that the command torque and rotor electrical velocity are constant, i.e., $\tilde{\tau} = \tilde{T}_0$ and $\omega_{re} = \Omega_{re}$, as well as $L_d \approx L_q$. These assumptions generally represent something of a "worst-case" scenario, since a time-varying torque reference and/or rotor electrical velocity, as well as a significant magnetic saliency, i.e., $L_q >> L_d$, will aid in parameter identification by providing additional excitation. Either directly, in the case of a varying torque command (and/or rotor velocity), or indirectly, via coupling between the command currents through the torque expression (5) in the presence of a significant magnetic saliency. Note that for the torque to remain constant in the presence of excitation introduced via the direct-axis dynamics, the quadrature-axis current must vary in an inverse manner, introducing additional excitation to the quadrature axis dynamics. Under these assumptions, we can rewrite the matrix $\mathbf{\Phi}_o(t)$ as follows,

$$\mathbf{\Phi}_o(t) = \begin{bmatrix} \tilde{i}_d^r(t) & C_\tau \tilde{T}_0 \\ \frac{d}{dt}\tilde{i}_d^r(t) & \Omega_{re}\tilde{i}_d^r(t) \\ -\Omega_{re}C_\tau \tilde{T}_0 & 0 \\ 0 & \Omega_{re} \end{bmatrix}. \quad (23)$$

where C_τ is a positive constant scalar, $C_\tau = \frac{4}{3P\Lambda_{PM}} > 0$. Additionally, we will neglect the reference filter $M(s)$ in our analysis as it has no effect on the results[3]. Without loss of generality, we may take $\tilde{i}_d^r = \sin(\omega t)$:

$$\mathbf{\Phi}_o(t) = \begin{bmatrix} \sin(\omega t) & C_\tau \tilde{T}_0 \\ \omega \cos(\omega t) & \Omega_{re}\sin(\omega t) \\ -\Omega_{re}C_\tau \tilde{T}_0 & 0 \\ 0 & \Omega_{re} \end{bmatrix}. \quad (24)$$

From Theorem 3, we may establish necessary and sufficient conditions for the regressor matrix (24) to be persistently exciting, by establishing conditions under which the rows of $\mathbf{\Phi}_o(t)$ in (24) are linearly independent. To do this, we will use the following theorem for checking linear independence of functions:

Theorem 4. *(Derivative Test [34]): Assume that the $1 \times p$ real-valued continuous functions $\vec{f}_1(t), \vec{f}_2(t), \cdots, \vec{f}_n(t)$ have continuous derivatives up to order $(n - 1)$ on the interval $[t_1, t_2]$. Let $\mathbf{F}$ be the $n \times p$ matrix with $\vec{f}_i(t)$ as its ith row, and let $\mathbf{F}^{(k)}$ be the kth derivative of $\mathbf{F}$. If there exists some t_0 in (t_1, t_2) such that the $n \times np$ matrix*

$$\left[\mathbf{F}(t_0) \vdots \mathbf{F}^{(1)}(t_0) \vdots \mathbf{F}^{(2)}(t_0) \vdots \cdots \vdots \mathbf{F}^{(n-1)}(t_0) \right]$$

has rank n, then the functions, $\vec{f}_i(t)$, are linearly independent on the interval $[t_1, t_2]$ over the field of reals.

---

[3]Given a persistently exciting u with $\dot{u}$ bounded, and a stable, minimum phase, proper transfer function $M(s)$, it follows that $y = M(s)u$ is also persistently exciting [1].

Since we are interested in sinusoidal inputs, we will consider $t_0 \in [0, \frac{2\pi}{\omega}]$. Applying Theorem 4 to (24), we take $t_0 = \frac{\pi}{2\omega}$ and compute:

$$\det\left(\left[\boldsymbol{\Phi}_o(t_0) \ \dot{\boldsymbol{\Phi}}_o(t_0)\right]\right) = -C_\tau \tilde{T}_0 \omega^2 \Omega_{re}^3. \qquad (25)$$

We conclude that the rows of $\boldsymbol{\Phi}_o(t)$ are linearly independent on $[0, \frac{2\pi}{\omega}]$, and $\boldsymbol{\Phi}(t, \vec{e}_i^r)$ is therefore persistently exciting, provided that:

1) the direct-axis command current, $\tilde{i}_d^r$, has at least one sinusoidal component (i.e., $\omega \neq 0$),
2) the command torque is non-zero, $\tilde{T}_0 \neq 0$,
3) the rotor (electrical) velocity is non-zero, $\Omega_{re} \neq 0$.

Remark: It should be noted that, in practice, it is important to normalize the rows of the regressor matrix such that the peak values are all around unity. Otherwise, the wide range of machine parameters, which are separated by orders of magnitude, will lead to convergence issues due to poor numerical conditioning. Note that this scales the corresponding parameter estimates as well.

Remark: When the rotor speed is not constant, but changing slowly with respect to the electrical reference variables, the same analysis can be carried out following the analysis techniques used in robust adaptive control [1]. The assumption that the rotor speed is slowly varying is justified by the time-scale separation between the electrical and mechanical dynamics.

VI. SIMULATION RESULTS

A. Ideal Case

Simulations using Matlab/Simulink are used to validate the proposed SIC design for PMSMs. We present results for the ideal case first, which assumes a "continuous-time" controller implementation, no time delay, and noise-free stator current measurements. Additionally, the inverter is assumed to be ideal in that the sinusoidal voltage commands generated by the control algorithm are fed directly into the machine model.

The proposed control methodology is demonstrated in Figure 4, specifically constraining the system state (i.e., the stator
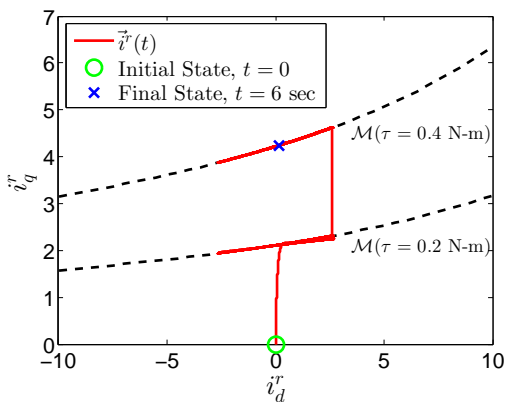

Fig. 4. Simulation result demonstrating state-trajectory convergence to the desired constant-torque manifolds using the proposed adaptive control design methodology with a step change in the commanded torque from 0.2 N-m to 0.4 N-m at a fixed rotor speed of 2000 RPM.

currents) to manifolds, $\mathcal{M}$, which correspond to a constant torque output (i.e., zero regulated output error). The adaptive controller is initialized with mismatched parameters, and a step-change in the command torque occurs 3 seconds into the simulation. Machine parameters which exaggerate the curvature of the manifolds were selected for the purpose of demonstrating the effectiveness of the proposed methodology.

The simulation results presented in Figure 5 demonstrate the stagnation of the parameter estimates when there is a lack of persistent excitation ($t \leq 0.75$ sec). Inspection of Fig. 5 reveals that, initially, when the direct-axis current and output torque commands are zero, the parameters fail to fully converge, as expected. Additionally, while there is partial convergence at 0.25 seconds due to excitation provided by the step change in command torque, the resistance and direct-axis inductance estimates do not converge quickly and fully until the excitation signal is added at 0.75 seconds. Finally, the black arrows in the "zoomed" plots in Fig. 5 point out overshoot in the torque resulting from the lack of parameter convergence.
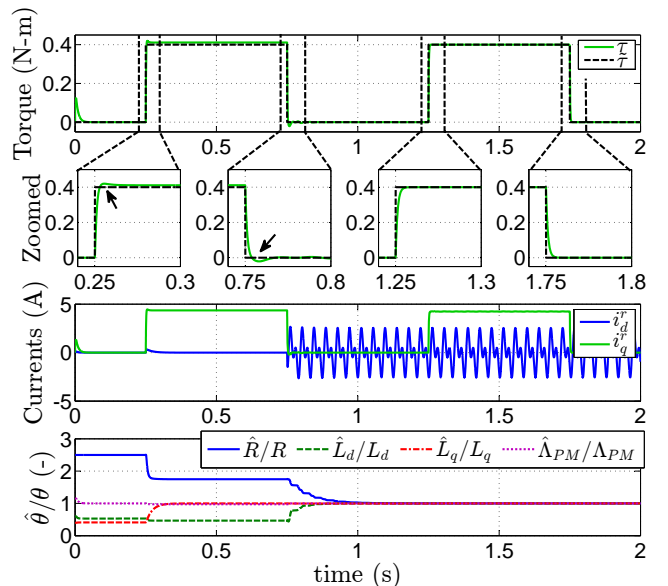

Fig. 5. Simulation of an ideal implementation of the proposed SIC design for PMSMs demonstrating parameter stagnation due an initial lack of persistent excitation, and the improvement resulting from the introduction of the excitation signal at 0.75 seconds.

B. Sampled-data Implementation: Time Delay and Compensation

The experimental implementation of the proposed control algorithm must take into account the sampled-data nature of its execution on a microprocessor. In particular, sampling of stator currents and encoder measurements is synchronized with a center-based pulse-width modulation (PWM) structure to prevent the pickup of electromagnetic interference (EMI) generated by switching transitions during sampling. A consequence of this synchronization is that it leads to a one-switching-period delay between sampling measurements and updating duty cycles, as depicted in Figure 6.
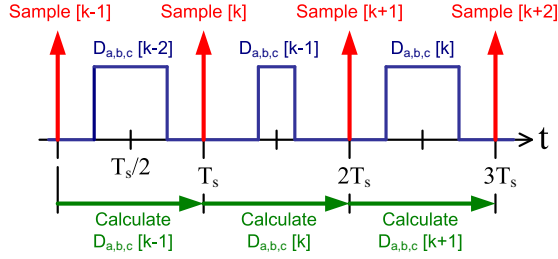
Fig. 6.   Timing sequence of digital controller implementation.

The presence of this time-delay will impose limits on control gains, K_{pd} and K_{pq}. Additionally, the use of reference-frame advancing in the inverse Park transform is required, as the rotor angular displacement during the delay interval can be significant. This discrepancy between the rotor position at the beginning and at the end of a sample period can lead to instability and parameter drift in the adaptive controller. To compensate for this angular displacement, the rotor position, θ_{re}, at the center of the next sample period is predicted assuming that the rotor velocity, ω_{re}, is constant over the sample period, T_s:

$$\hat{\theta}_{re}[k+1] = \theta_{re}[k] + \frac{3}{2}\omega_{re}[k]T_s, \qquad (26)$$

where $k = 1, 2, 3...$ represents the discrete time indices. The predicted rotor position (26) is then used to compute the inverse Park transform in the discrete-time controller implementation.

To demonstrate the impact that this rotor angle discrepancy has on the parameter estimator, we include the simulation results in Figure 7. A triggered subsystem is used in Simulink to capture the sampled-data nature of the experimental implementation. The subsystem is triggered by an inverter model which is using center-based PWM at a rate of 8 kHz, like the experimental set-up, and includes a one-time-step delay. The simulation which produced Fig. 7 *did not* include reference-frame advancing based on (26). The switching-σ modification bounds the parameter estimates. However, inspection of Fig. 7 clearly reveals that the parameter estimates (resistance and quadrature-axis inductance in particular) are sensitive to this rotor angle discrepancy resulting from the time delay present in the sampled-data implementation.
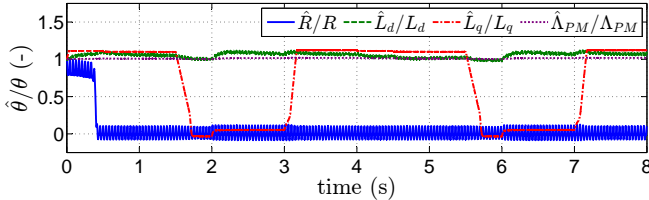

Fig. 7.   Simulation of sampled-data system *without* reference-frame advancing at a speed of 2000 RPM with step changes in command torque (the same as in Fig. 8), leading to poor parameter estimator performance.

For comparison (to Fig. 7), we provide simulation results which include reference frame advancing based on (26) in Figures 8 and 9. This simulation uses the same Simulink code
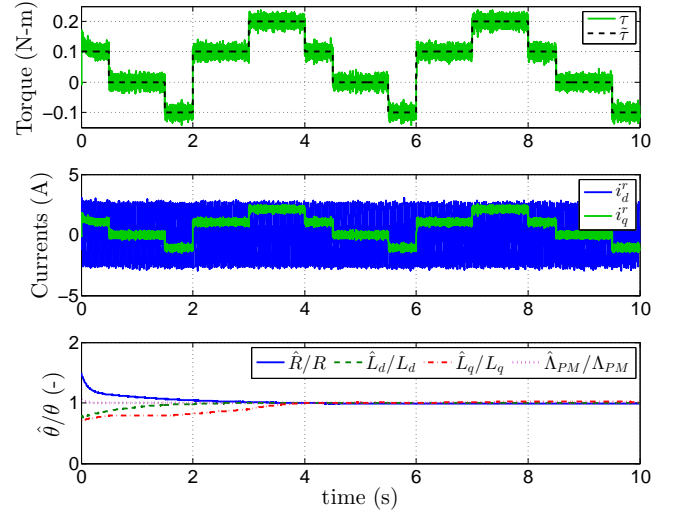
Fig. 8.   Simulation of the proposed adaptive control design in a sampled-data scenario *with* reference-frame advancing based on (26) and measurement noise at a rotor speed of 2000 RPM.

that was used to generate the experimental code using Real-time Workshop. It should be noted that the inverter model in this result did not include dead-time effect [13]. The "nominal" parameters provided in Table II were used in the PMSM model. Inspection of Fig. 8 reveals that the algorithm works as intended under sampled-data conditions, provided that the time-delay is compensated via reference-frame advancing.

Finally, the simulation results provided in Figure 9 demonstrate operation under field-weakening [12], in which a negative direct-axis current is commanded to reduce the EMF generated by the permanent magnets and extend the speed range of the machine under voltage constraints. This is accomplished by simply adding a negative (field-weakening) direct-axis current
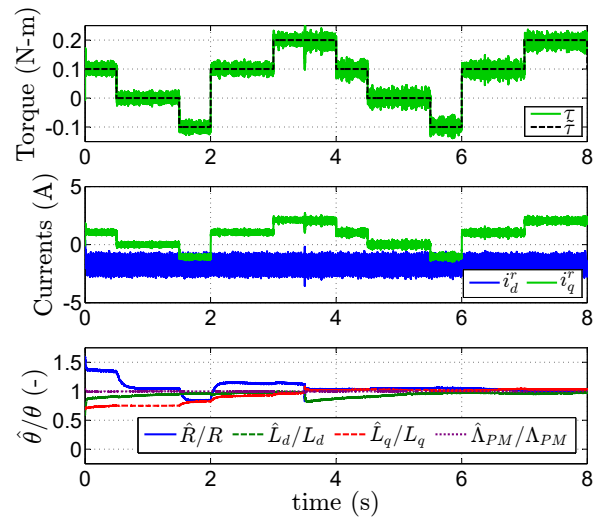
Fig. 9.   Simulation of the proposed adaptive control design under field weakening (i.e., the is a negative offset in the direct-axis current) in a sampled-data scenario *with* reference-frame advancing based on (26) and measurement noise at a rotor speed of 2000 RPM, with a step change in machine parameters at 3.5 sec.

offset to the excitation signal. The simulation results in Fig. 9 also demonstrate the ability to track a step change in parameters which occurs 3.5 seconds into the simulation. Note that, while the excitation signal can be reduced in amplitude, as it was in Fig. 9 (in comparison to Fig. 8), a smaller excitation signal will slow down parameter convergence (for equivalent gains) and will cease to provide any benefit when the excitation signal amplitude approaches the noise levels of the system.

VII. EXPERIMENTAL VALIDATION

A. Test Machine Parameters

For simulation and comparison purposes, the "nominal" test machine parameters were determined offline using standard techniques. The (DC) stator resistance was measured with a Digital Multi-Meter, inductance with an Agilent E4980A LCR meter, and the permanent magnet flux linkage was identified using an open-circuit test and a linear regression. These nominal parameters, denoted by an overbar, are provided in Table II. We must emphasize that we *do not* expect that the parameter estimates provided by our adaptive controller will converge to these values, since they are not necessarily the *true* physical parameters of the machine. For instance, the resistance measured with a DMM does not account for skin-effect and inverter losses, while the formation of eddy currents in the rotor iron can lead to an error in the measured inductance when using a standard LCR meter.

TABLE II
"NOMINAL" TEST MACHINE PARAMETERS.

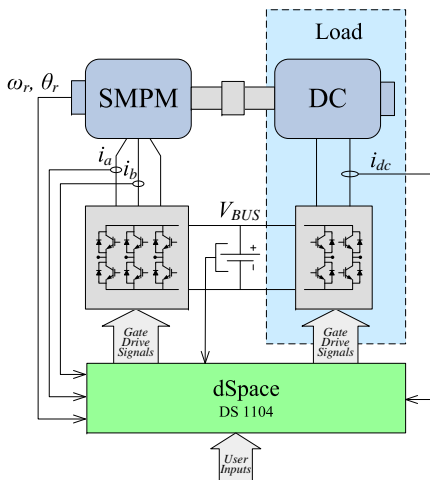| Parameter	Value
Resistance, $\bar{R}$	109 mΩ
Direct-axis self-inductance, $\bar{L}_d$	192 μH
Quadrature-axis self-inductance, $\bar{L}_q$	212 μH
PM Flux Linkage, $\bar{\Lambda}_{PM}$	12.579 mV-s
No. of Poles, P	10

B. Description of the Experimental Set-up

Fig. 10. Experimental setup.

The proposed robust adaptive control algorithm has been implemented on experimental hardware using a dSPACE DS1104 controller board, and the test machine (Table III) is a 3-phase, 10-pole, 250 watt SMPM machine from MOTOR-SOLVER with "nominal" parameters (denoted by the over bar) listed in Table II. A 250-watt DC machine from the same manufacturer serves as the load for the SMPM machine.

A power MOSFET inverter is used to drive the motors with a switching frequency of 8 kHz and a bus voltage of 42 VDC. First-harmonic dead-time compensation is used to mitigate the voltage discrepancy resulting from the insertion of "dead-time" in the gate-drive signals [35]. Duty cycles are calculated using conventional pulse-width-modulation, and the ADC sampling is synchronized with, and offset from, the center-based PWM signals to avoid sampling during a switching event (as discussed in the previous section). Note that the sampling rate of our controller is also 8 kHz due to this synchronization of switching and sampling. Finally, position/velocity feedback is provided by a 2048-line (per revolution) incremental encoder.

TABLE III
MANUFACTURER MACHINE RATINGS.

Test Motor		Load Motor	
Type:	PM Brushless	Type:	DC
No. Phases:	3	No. Phases:	N.A.
V/I:	42 V/5.7 A	V/I:	42 V/6 A
Max. Speed:	4000 RPM	Max. Speed:	4000 RPM
Rated Power:	250 W	Rated Power:	250 W

C. Experimental Results

Since mechanical torque was not measured during these experiments, the quadrature stator current (in the rotor reference frame) is used to evaluate the transient performance of the proposed torque regulator in addition to the estimated electromagnetic torque (27), which can vary with the parameter estimates:

$$\hat{\tau} = \frac{3P}{4}\left[\left(\hat{L}_d - \hat{L}_q\right)i_d^r + \hat{\Lambda}_{PM}\right]i_q^r. \qquad (27)$$

It should be noted that, since torque is not measured directly, accurate knowledge of the permanent magnet flux linkage, as well as the direct and quadrature self-inductance, is required for accurate torque regulation. Torque steps, used to evaluate the performance of the proposed adaptive torque regulator, are provided in Figures 11 and 12.

In Fig. 11 we see that the estimated torque tracks the commanded value very well without any undesirable jumps or drifting in the parameter estimates. A direct-axis current reference of $\tilde{i}_d^r = 1.5\sin(150t) + 1.5\sin(300t)$ amps provides excitation for parameter estimation. Note that the estimated parameter values have been normalized with respect to their "nominal" values in Table II, which are not necessarily the *true* values (which are unknown), to facilitate plotting on the same axis for comparison.

A feature of the proposed adaptive controller design is that its closed-loop transient response remains consistent across a wide range of operating points. To demonstrate this, torque
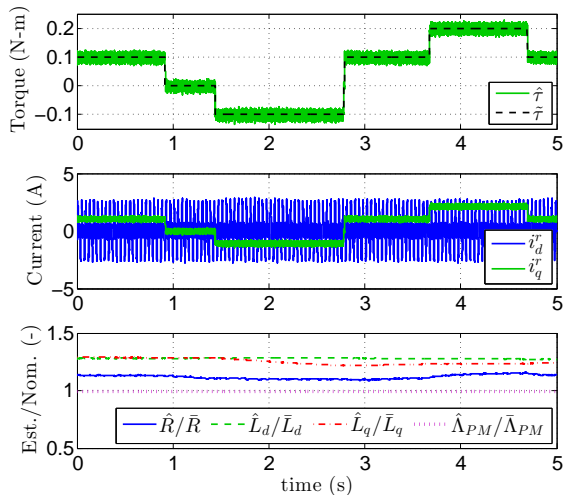
Fig. 11. Experimental torque steps with adaptation on at 2000 rpm.

Fig. 13. Experimental adaptive parameter estimator for a constant torque command of 0.2 N-m at a fixed rotor speed of 2000 RPM demonstrating transient characteristics of the parameter estimator as well as asymptotically vanishing torque perturbation due to the excitation signal.

steps from 0 to 0.4 N-m were performed at 2500, 1200, and 0 RPM, and are plotted in Fig. 12. Note that the responses overlay, indicating that the controller is performing as expected. Additionally, the "ripple" or "noise" which can be seen in the signals is expected, and is largely due to the non-ideal slotting effects in the machine. Furthermore, the decision to stop at 2500 RPM is based on the fact that the voltage-constraints of the inverter are encountered at around 3000 RPM. Field-weakening may be used to extend operation to higher speeds by adding the appropriate negative offset to the excitation signal (i.e., including a negative DC bias in the persistently exciting direct-axis reference current).

As discussed earlier in this paper, the proposed adaptive control design achieves the simultaneous identification and control objective in that it allows excitation signals to be introduced for parameter identification whose impact on the output is minimized (asymptotically, in the case of our design). This property is demonstrated in Figure 13, in which the transient response of the experimental adaptive parameter

estimator for a constant torque command of 0.2 N-m at a fixed rotor speed of 2000 RPM is plotted. Initially, the parameter values are intentionally mismatched such that the excitation signal disturbs the torque output. Inspection of Fig. 13 reveals that, as the estimates converge, the disturbance caused by the excitation signal vanishes, as expected.

To gauge the performance of our parameter identification, we recorded the steady-state values of the estimated parameters over a range of operating points in which the parameters are all identifiable (i.e., non-zero rotor speed and torque command). Inspection of the results in Figure 14 indicate that the parameter estimation is working very well overall. The resistance estimate is fairly consistent across rotor speed, but increases slightly with the torque command, potentially due to temperature rise. The estimated direct-axis inductance and permanent magnet flux linkage are very consistent across rotor speed and torque, as expected. The drop in the estimated permanent magnet flux linkage at 500 RPM is likely due to the increasing impact of the dead-time effect at lower speeds (which generally correspond to smaller stator voltages). Finally, the wider variation in the quadrature-axis inductance was anticipated, as this parameter was observed to be particularly sensitive to encoder misalignment while tuning the experimental controller. This behavior was also observed in simulations which introduced a fixed rotor angle offset error. However, we have found that the impact of this variation on the controller performance (i.e., output regulation) is negligible.

Still, it is worth noting that the quadrature-axis inductance estimate seems to improve at higher speeds, yielding a nearly flat trend at 2000 RPM (see Fig. 14), and estimates around the same value as the direct-axis inductance. This is to be expected as our test machine was a surface-mount permanent magnet (SMPM) machine which, characteristically, have a negligible
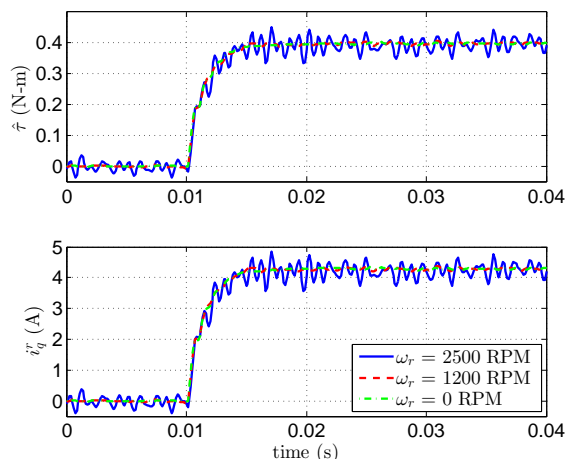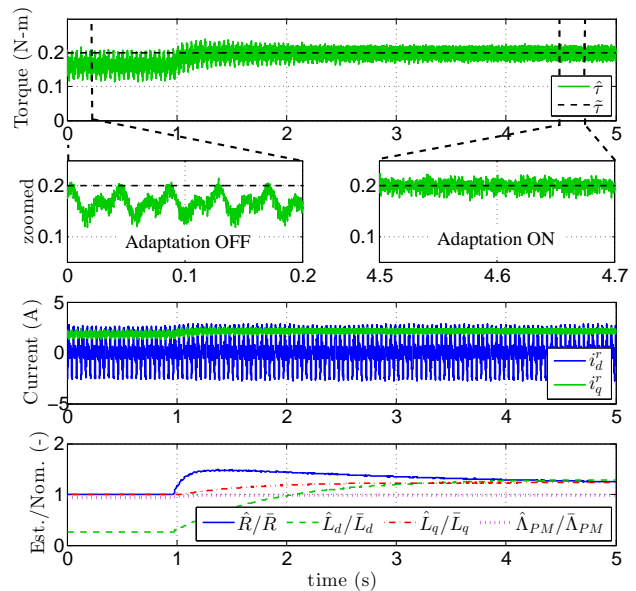

Fig. 12. Experimental transient responses of estimated torque (*top*) and measured quadrature-axis current (*bottom*) across a wide range of rotor speeds.
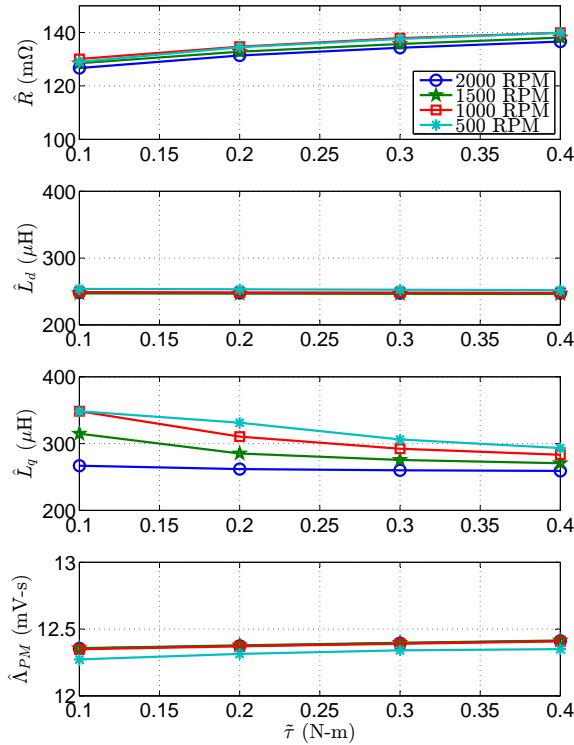
Fig. 14. Experimental characterization of steady-state parameter estimates over a wide range of rotor speeds and torque commands.

magnetic saliency (i.e., it is commonly assumed that $L_d \approx L_q$ for SMPM machines). Recall that, under a constant torque command and rotor speed, the third row of the regressor, which relates to the quadrature inductance estimate (see equation (24)), is dependent on the following term: $-\Omega_{re}C_\tau \tilde{T}_0$. At a minimum, a nonzero torque command, $\tilde{T}_0$, and rotor speed, Ω_{re}, are needed for the regressor to be persistently exciting, otherwise the third row of the regressor will be all zeros and the estimate of quadrature-axis inductance will stagnate. Practically, it is expected that the estimate of the quadrature-axis inductance, L_q, will suffer from drifting in the presence of modeling errors, such as encoder misalignments, at low speeds and/or torque commands. This may explain why the estimate of L_q seems to improve at high speeds, as well as higher torque commands, as observed in Fig. 14.

VIII. CONCLUSION

This paper extended results from [28], which presented a new robust adaptive torque regulating controller for SMPM machines that estimates resistance, inductance, and permanent magnet flux linkage online. The adaptive controller for PMSMs presented was derived using Lyapunov's stability theorem, and a robust modification to the derived adaptive law is used to ensure closed-loop stability in the presence of unmodeled disturbances. The control law utilizes a combination of adaptively-tuned feedforward (to achieve zero steady-state error), $d-q$ decoupling (to improve transient response), and proportional feedback (to add robustness to disturbances) terms. Overactuation of the system is exploited to simultaneously achieve parameter convergence and torque

regulation. Excitation for parameter identification is introduced via the direct-axis current reference input, and necessary conditions for persistent excitation were discussed. Simulation results verifying the performance of the control design were presented. Finally, remarks specific to experimental implementation challenges, and experimental results validating the performance of the proposed design, were discussed.

If desired, machine parameter may be identified during startup. The excitation may then be turned off after a commissioning phase, and the adaptation stopped by setting the adaptation gain to be the zero matrix. However, by keeping the adaptation and excitation active, the controller will be able to compensate for parameter variations, particularly in the inductances and PM flux linkage whose variations directly impact the accuracy of the unmeasured regulated torque output. Finally, the magnitude of the excitation signal can be reduced when operating near the voltage / current limits of the machine, shutting off the excitation and adaptation completely when the amplitude approaches the noise level of the system. The main impact of reducing the amplitude of the excitation signal is slower parameter convergence, while drifting may occur when the amplitude reaches the noise level.

APPENDIX A
PROOF OF THEOREM

Consider the matrix function $\boldsymbol{\Phi}(t) : \mathbb{R}_{\geq 0} \mapsto \mathbb{R}^{n \times m}$ where the elements of $\boldsymbol{\Phi}(t)$ are bounded for all time, t.

"If"

Assume that regressor matrix $\boldsymbol{\Phi}(t)$ is persistently exciting. It follows that there exist $\alpha_1, \alpha_0, T > 0$ such that

$$\alpha_1 \mathbf{I} \geq \int_t^{t+T} \boldsymbol{\Phi}(\sigma)\boldsymbol{\Phi}^\top(\sigma)d\sigma \geq \alpha_0 \mathbf{I}, \ \forall \ t \geq 0.$$

From Theorem 5-1 in [34], the Gramian matrix, $\mathbf{W}(t, t+T)$, is positive definite, i.e.

$$\mathbf{W}(t, t+T) \triangleq \int_t^{t+T} \boldsymbol{\Phi}(\sigma)\boldsymbol{\Phi}^\top(\sigma)d\sigma \geq \alpha_0 \mathbf{I},$$

if, and only if, the rows of $\boldsymbol{\Phi}(\sigma)$ are linearly independent on $[t, t+T]$. Thus, it follows that *if* $\boldsymbol{\Phi}(t)$ is persistently exciting, *then* the rows of $\boldsymbol{\Phi}(t)$ are linearly independent on $[t, t+T]$.

"only if"

Assume that the rows of $\boldsymbol{\Phi}(t)$ are linearly independent on $[t, t+T]$ for all $t \geq 0$ and some $T > 0$. It follows that the Gramian matrix is positive definite; i.e., there exists $\alpha_0 > 0$ such that

$$\mathbf{W}(t, t+T) \geq \alpha_0 \mathbf{I} \ \forall \ t \geq 0.$$

Furthermore, since the elements of $\boldsymbol{\Phi}(t)$ are bounded for all time, t, it follows that there exists $\alpha_1 > 0$ such that

$$\alpha_1 \mathbf{I} \geq \mathbf{W}(t, t+T) \geq \alpha_0 \mathbf{I} \ \forall \ t \geq 0.$$

Thus, *if* the rows of $\boldsymbol{\Phi}(t)$ are linearly independent on $[t, t+T]$ for all $t \geq 0$ and some $T > 0$, *then* $\boldsymbol{\Phi}(t)$ is persistently exciting.

$\boxtimes$

REFERENCES

[1] P. Ioannou and J. Sun, *Robust Adaptive Control*. New Jersey: Prentice Hall, 1996.

[2] A. Feldbaum, "Dual control theory," *Automation and Remote Control*, vol. 21, no. 9, pp. 874–1039, 1960.

[3] K. Astrom and B. Wittenmark, *Adaptive Control*. New York: Dover, 2nd ed., 2008.

[4] H. Genceli and M. Nikolaou, "New approach to constrained predictive control with simultaneous model identification," *AIChE Journal*, vol. 42, no. 10, pp. 2857–2868, 1996.

[5] G. Marafioti, R. Bitmead, and M. Hovd, "Persistently exciting model predictive control using fir models," in *International Conference Cybernetics and Informatics*, 2010.

[6] J. Rathouský and V. Havlena, "Mpc-based approximate dual controller by information matrix maximization," *International Journal of Adaptive Control and Signal Processing*, vol. 27, no. 11, pp. 974–999, 2013.

[7] I. Kolmanovsky and D. Filev, "Optimal finite and receding horizon control for identification in automotive systems," in *Identification for Automotive Systems*, Lecture Notes in Control and Information Sciences, pp. 327–348, Springer London, 2012.

[8] A. Weiss and S. Di Cairano, "Robust dual control mpc with guaranteed constraint satisfaction," in *Decision and Control (CDC), 2014 IEEE 53rd Annual Conference on*, pp. 6713–6718, Dec 2014.

[9] F. Leve and M. Jah, "Spacecraft actuator alignment determination through null motion excitation," in *Proceedings of 62nd International Astronautical Congress*, 2011.

[10] A. Weiss, F. Leve, I. Kolmanovsky, and M. Jah, "Reaction wheel parameter identification and control through receding horizon-based null motion excitation," in *Advances in Estimation, Navigation, and Spacecraft Control*, pp. 477–494, Springer Berlin Heidelberg, 2015.

[11] Y. Chen and J. Wang, "Adaptive vehicle speed control with input injections for longitudinal motion independent road frictional condition estimation," *Vehicular Technology, IEEE Transactions on*, vol. 60, pp. 839–848, March 2011.

[12] R. Krishnan, *Permanent Magnet Synchronous and Brushless DC Motor Drives*. Boca Raton: CRC Press, 2009.

[13] B. Bose, *Modern Power Electronics and AC Drives*. New Jersey: Prentice Hall PTR, New Jersey, 2002.

[14] R. Marino, S. Peresada, and P. Tomei, "Nonlinear adaptive control of permanent magnet step motors," *Automatica*, vol. 31, no. 11, pp. 1595 – 1604, 1995.

[15] S. D. Gennaro, "Adaptive output feedback control of synchronous motors," *International Journal of Control*, vol. 73, no. 16, pp. 1475–1490, 2000.

[16] A. Loria, G. Espinosa-Prez, and S. Avila-Becerril, "Global adaptive linear control of the permanent-magnet synchronous motor," *International Journal of Adaptive Control and Signal Processing*, vol. 28, no. 10, pp. 971–986, 2014.

[17] V. Petrovic, R. Ortega, A. Stankovic, and G. Tadmor, "Design and implementation of an adaptive controller for torque ripple minimization in pm synchronous motors," *Power Electronics, IEEE Transactions on*, vol. 15, pp. 871–880, Sep 2000.

[18] S. Underwood and I. Husain, "Online parameter estimation and adaptive control of permanent-magnet synchronous machines," *IEEE Transactions on Industrial Electronics*, vol. 57, pp. 2435 – 2443, July 2010.

[19] S. Ichikawa, M. Tomita, S. Doki, and S. Okuma, "Sensorless control of permanent-magnet synchronous motors using online parameter identification based on system identification theory," *IEEE Transactions on Industrial Electronics*, vol. 53, pp. 363 – 372, April 2006.

[20] A. Blauch, M. Bodson, and J. Chiasson, "High-speed parameter estimation of stepper motors," *Control Systems Technology, IEEE Transactions on*, vol. 1, pp. 270–279, Dec 1993.

[21] R. Delpoux, M. Bodson, and T. Floquet, "Parameter estimation of permanent magnet stepper motors without mechanical sensors," *Control Engineering Practice*, vol. 26, no. 0, pp. 178 – 187, 2014.

[22] Y. A.-R. I. Mohamed, "Design and implementation of a robust current-control scheme for a pmsm vector drive with a simple adaptive disturbance observer," *IEEE Transactions on Industrial Electronics*, vol. 54, pp. 1981 – 1988, August 2007.

[23] K. Liu, Q. Zhang, J. Chen, Z. Zhu, and J. Zhang, "Online multiparameter estimation of nonsalient-pole pm synchronous machines with temperature variation tracking," *IEEE Transactions on Industrial Electronics*, vol. 58, pp. 1776 – 1788, May 2011.

[24] H. Melkote and F. Khorrami, "Nonlinear adaptive control of direct-drive brushless dc motors and applications to robotic manipulators,"

[25] L. Liu and D. Cartes, "Synchronisation based adaptive parameter identification for permanent magnet synchronous motors," *IET Control Theory Applications*, vol. 1, pp. 1015 – 1022, July 2007.

[26] H. Kim and R. Lorenz, "Improved current regulators for ipm machine drives using on-line parameter estimation," in *Industry Applications Conference, 2002. 37th IAS Annual Meeting. Conference Record of the*, vol. 1, pp. 86–91, Oct 2002.

[27] K.-W. Lee, D.-H. Jung, and I.-J. Ha, "An online identification method for both stator resistance and back-emf coefficient of pmsms without rotational transducers," *IEEE Transactions on Industrial Electronics*, vol. 51, pp. 507 – 510, April 2004.

[28] D. M. Reed, J. Sun, and H. F. Hofmann, "A robust adaptive controller for surface-mount permanent magnet synchronous machines," in *American Control Conference (ACC), 2014*, pp. 5236–5241, June 2014.

[29] F. Blaschke, "The principle of field orientation as applied to the new transvector closed loop control for rotating field machines," *Siemens Rev.*, vol. 39, pp. 217–220, May 1972.

[30] R. Park, "Two-reaction theory of synchronous machines, generalized method of analysis - part 1," *A.I.E.E. Transactions*, vol. 48, pp. 81–95, 1929.

[31] P. Krause, O. Wasynczuk, and S. Sudhoff, *Analysis of Electric Machinery and Drive Systems*. New Jersey: John Wiley and Sons, 2nd ed., 2002.

[32] J.-J. E. Slotine and W. Li, *Applied Nonlinear Control*. New Jersey: Prentice Hall, 1991.

[33] A. Loria, E. Panteley, D. Popovic, and A. R. Teel, "δ-persistency of excitation: a necessary and sufficient condition for uniform attractivity," in *Decision and Control, 2002, Proceedings of the 41st IEEE Conference on*, vol. 3, pp. 3506–3511 vol.3, Dec 2002.

[34] C.-T. Chen, *Linear System Theory and Design*. New York: Holt, Rhinehart, and Winston, 1984.

[35] D. Reed, K. Zhou, H. Hofmann, and J. Sun, "A stator current locus approach to induction machine parameter estimation," in *Transportation Electrification Asia-Pacific (ITEC Asia-Pacific), 2014 IEEE Conference and Expo*, pp. 1–6, Aug 2014.

Mechatronics, IEEE/ASME Transactions on, vol. 4, pp. 71–81, Mar 1999.